Cogging Torque Minimization of Dual Rotor Axial Flux Permanent Magnet Brushless DC Motor Using Magnet Shifting Technique

Amit N. Patel[1,*]

ARTICLE INFO

Article history:
Received: 26 January 2023
Revised: 1 May 2023
Accepted: 28 May 2023

Keywords:
Magnet shifting
Permanent magnet motors
FEA
Cogging torque

ABSTRACT

The reduction of cogging torque of a dual rotor axial flux brushless DC (AF-BLDC) motor through rotor side design variation is presented in this article. Cogging torque minimization is highly desirable as it deteriorates torque quality of motor. For exact electromagnetic field analysis three-dimensional(3-D) finite element method is used. In performance evaluations, the initially designed axial flux brushless DC motor is used as the reference motor. Magnet shifting technique is performed on rotor side of an improved motor with an objective of cogging torque minimization. Using the 3-D finite element method, extensive research has been done to examine the effects of magnet shifting on the average torque and cogging torque of the AF-BLDC motor. By comparison between reference and improved ones the validity of the analysis results is also clarified. The magnet shifting technique is found to be successful in reducing cogging torque of AF-BLDC motors since the peak cogging torque value is reduced by 44.75%.

1. INTRODUCTION

Permanent magnet motors are used in a variety of applications in the current electrical motor market that call for efficient, a broad range of speed, small size, and quick response [1]-[3]. The main driver behind the widespread use of PMBLDC motors has been the development of semiconductor switches and high energy permanent magnet (PM) materials. PMBLDC motors are classified into two types based on their magnetic flux distribution: radial flux brushless dc (RF-BLDC) motors and axial flux brushless dc (AF-BLDC) motors [4]. Flux sets orthogonal to the motor shaft in RF-BLDC motors whereas, magnetic flux sets in axial direction i.e., parallel to the shaft of the motor in AF-BLDC motors. AF-BLDC motor with virtues such as excellent efficiency, better copper utilization, high power density, adjustable air gap length, compact structure and flat shape [5] are widely used for vehicular propulsion system, low-speed applications [6] and small direct-drive wind energy conversion systems [7], etc.

Torque ripple very crucial performance factor in applications that depend on torque quality. Hence, assessment of torque quality is important and is a challenging assignment in AF-BLDC motor. This is because torque density is to be considered with torque ripple in assessment. It is critical to comprehend the impact of high torque ripple as it is more dominating in low-speed range and results in vibration and noise [8]. Torque quality improvement for performance enhancement is one of the key research interests of many researches. There are four sources that lead to generation torque ripple i.e., cogging torque (CT), dc link voltage and fluctuation in delay time of inverter, phase excitation switching, distorted counter EMF and stator current waveform. CT is one of the major components that contribute to torque ripple in permanent magnet motors. It originates because of the interaction of stator teeth and PM [9]. Hence, it is an inherent property of permanent magnet motor. Cogging torque is independent of load current and is proportional to reluctance variation and PM flux. To improve the overall performance of AF-BLDC motors, it is important to improve torque quality and one of the methods to achieve that is by reducing CT. Because every change in control technique will result in a reduction in efficiency, reducing CT through design optimization is always desirable. Several approaches have been proposed for minimization of CT of BLDC motors like adding dummy slots, skewing of rotor and/or stator, shaping of magnet pole, selecting proper slot/pole ratio, slot opening optimizing, re-shaping and/or notching of stator tooth, changing air-gap length, notching of magnets, pole arc variation, stepped stator slot, slot opening shifting, dual notching and etc. [10]–[19]. Some of these approaches are directly applicable in AF-BLDC motor. But cost and manufacturability are crucial factors, as low cost and manufacturable approaches are desirable. One of the efficient techniques for CT reduction in AF-BLDC motors is magnet skewing [20,21]. One disadvantage of the magnet skewing technique is the formation of undesirable axial thrust [22]. CT can be

[1]*Department of Electrical Engineering, Institute of Technology, Nirma University, Ahmedabad, Gujarat, India - 382481.*
**Corresponding author:* Amit N. Patel; E-mail: amit.patel@nirmauni.ac.in.

reduced in AF-BLDC motors by stator side adjustments such as skewed slot opening, relative displacement of slot opening, and slot opening variation [23]. In AF-BLDC motor CT is influences by magnet pole arc. Magnet pole arc optimization technique reduces CT with compromise in profile of back EMF and motor output. Magnet notching technique is preferred for the reduction of CT of sandwiched stator AF-BLDC motor [23]. Stator side modification in an AF-BLDC motor is neither preferred and nor practical approach as it increases the manufacturing complexity which results in increment of manufacturing cost of the motor. Whereas, CT minimization by rotor side modifications is desirable in AF-BLDC motor as it is cost effective and more practical compared to that of stator modification methods.

In this work, the suggested magnet shifting technique addresses the reduction in CT of the AF-BLDC motor. Effect of shifting of magnet on CT profile and back EMF profile are addressed. To address electromagnetic problems and simulate approaches, three-dimensional finite element analysis (FEA) is employed. This method is easily implementable and doesn't incur any additional costs. Section 2 describes the fundamentals of CT and its reduction. Section 3 provides brief summary of reference dual rotor AF-BLDC motor. Section 4 explains the magnet shifting approach. Section 5 discusses the simulation and results of the proposed technique. Section 6 finally presents the conclusion.

2. BASICS OF COGGING TORQUE

Cogging torque is present even without supplying power to the motor. It is generated due to interactions between the anisotropy created by slots and PM mounted on the rotor. During rotation, magnetic field energy changes because of this anisotropy and cogging torque is produced according to following equation (1) where W_r is magnetic field energy and θ_r is rotor angle.

$$T_{cogg} = -\frac{\partial W_r}{\partial \theta_r} \tag{1}$$

Although cogging torque does not add to the total amount of work done, it interferes with the electromagnetic torque and results innto inferior torque quality. As it is outcome of the interplay between permanent magnet on rotor side and the opening of stator slots, cogging torque period can be represnted from the number of rotor poles and stator slots. The resultant CT is sum of harmonic torques on account of interaction between the edges of each magnet and the slot openings. CT periods (N_p) contained in a single rotor revolution can be derived from equation 2. This important indication provides information on the spatial displacement of the fundamental CT waveforms [25].

$$N_p = LCM\{S_S, 2p\} \tag{2}$$

Where, S_S is the number of stator slots and $2p$ is the number of poles. The spatial period of the CT waveform, T_p can be expressed by the following relationship:

$$T_p = \frac{2\pi}{LCM\{S_S, 2p\}} \tag{3}$$

where, T_p is inversely proportional to N_p as illustrated in equation 3. Maximum value of CT is achieved when the phases of elementary torques are same, that means value of N_p is minimum (N_p = 1 in equation 3). The resultant CT value will be minimum if the elementary torques are different phases. And higher values of N_p lead to reduced value of CT due to the distribution of elementary torques along the slot pitch. Equation 4 represents the expression for CT waveform using Fourier series.

$$T_{cogg} = \sum_{i=1}^{\infty} T_p N_p i \sin\left(N_p i \alpha\right) \tag{4}$$

where, i is order of harmonics, α is relative displacement of motor and $T_p N_p i$ is Fourier coefficient. Many approaches are attempted to minimize the amplitude of the primary harmonics by focusing either on one of squared magneto-motive force (MMF) and permanence or by focusing on both quantities, as magnetic energy is a function of these physical quantities.

3. REFERENCE DUAL ROTOR AXIAL FLUX BLDC MACHINE

As shown in fig.1, this section describes the design of a reference machine for a three phase 250 W, 150 rpm dual rotor AF-BLDC motor for electrical vehicle applications. Initially designed AF-BLDC motor has one stator with 48 slots placed in between two 8 poles PM rotors. Stator core of the machine is made of M19 – 29 Gage cold rolled electrical steel martial with ring type winding. Whereas, rotor discs comprise rotor core made of the same M19 – 29 Gage material and poles made of NdFeB grade 50 to ensure better performance.

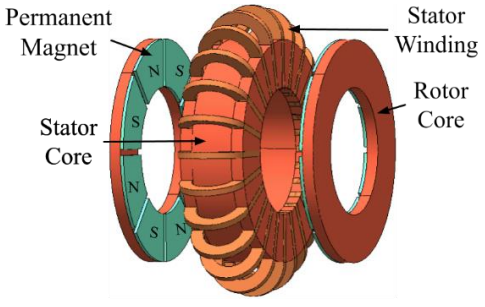

Fig. 1. Axial Flux BLDC Motor.

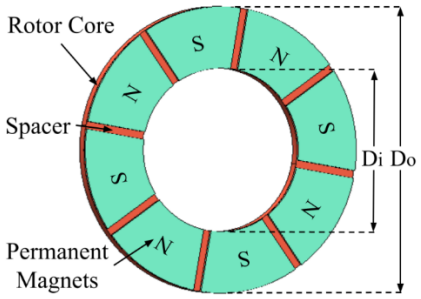

Fig. 2. Rotor disc of reference motor.

The following merits guided the selection of the PM materials:

i. Core & teeth size compatibility
ii. Working temperature resistant
iii. High magnetic flux density
iv. Cost & availability

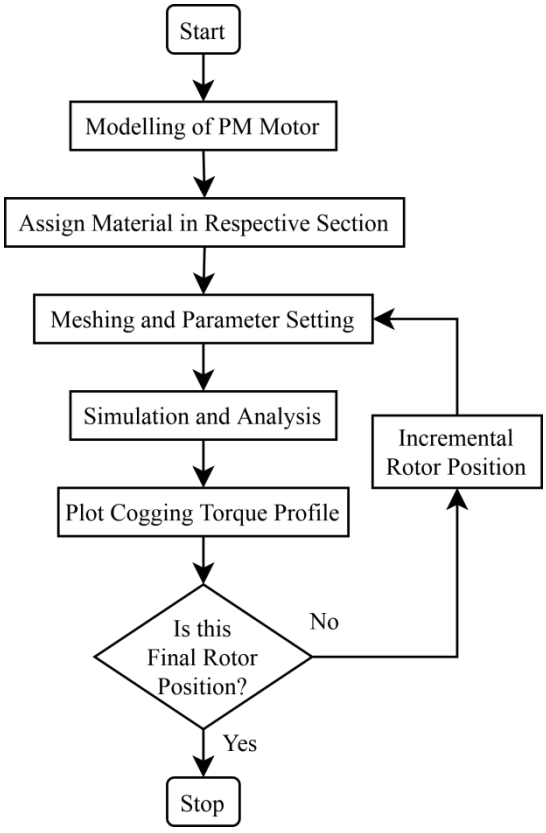

Fig. 3. Flow chart to obtain CT profile.

Specific magnetic loading, specific electric loading, stator current density, space factor, diametric ratio, slot-pole combination, assumed flux density in respective core section are few design variables assumed in motor design. The above-mentioned various design variables are appropriately assumed based on application requirements, availability of materials and manufacturability. The model that was originally designed serve as a benchmark for evaluating and analyzing performance. The initially intended motor is not subjected to any of the CT reduction procedures. Initial design has uniformly distributed magnets poles on each rotor. The improved model retains all the dimensions of reference motor except placement of permanent magnets on rotor disc. The significant design details for the reference motor are shown in Table I. Figure 2 shows one of the rotor discs with eight permanent magnet poles designed using NdFeB grade 50 type material and other different parts. For accurate electromagnetic field analysis, 3D modelling and simulation is considered in AF-BLDC motor. Commercially accessible finite element software is used for modelling and simulation. FEA is used for obtaining the CT at a particular rotor position. And this is iterated till the final rotor position is reached. Figure 3 show the flow chart for this process of obtaining the CT profile of designed and improved dual rotor AF-BLDC motor. It is observed that the CT variation is periodic w.r.t. rotor position because of motor's structural symmetry. The peak CT value of initially designed AF-BLDC motor is 5.43 N.m. as shown in Fig. 4.

Table 1. Details of initial motor

Parameters	Symbol	Unit	Value
No. of phase	N_{ph}	-	3
No. of slots	N_s	-	48
No. of poles	p	-	16
Outer dia.	D_o	mm	182
Inner dia.	D_i	mm	104
PM length	L_m	mm	2.7
Air-gap length	L_g	mm	0.5
PM remanence	B_r	T	1.2
Type of PM	-	Grade 50	NdFeB
Core material type	-	-	M19

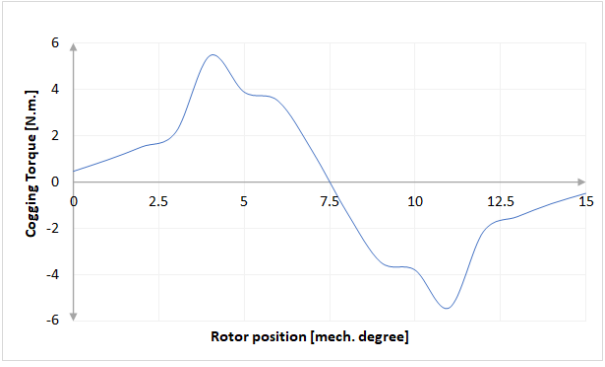

Fig. 4. CT profile of initially designed motor.

4. MAGNET SHIFTING TECHNIQUE

This section discusses the Magnet Shifting (MS) technique for CT reduction for a dual rotor AF-BLDC motors. Various design approaches for CT reduction of BLDC permanent magnet machines are listed in literature. CT is produced in AF-BLDC motors on account of interaction between flux and reluctance variation at air-gap. And it can be mitigated by reducing variation in air-gap reluctance. This section presents a new rotor with shifted magnets. If the ends of all the magnets are evenly spaced apart, overall CT represents the sum of the contributions from each magnet.

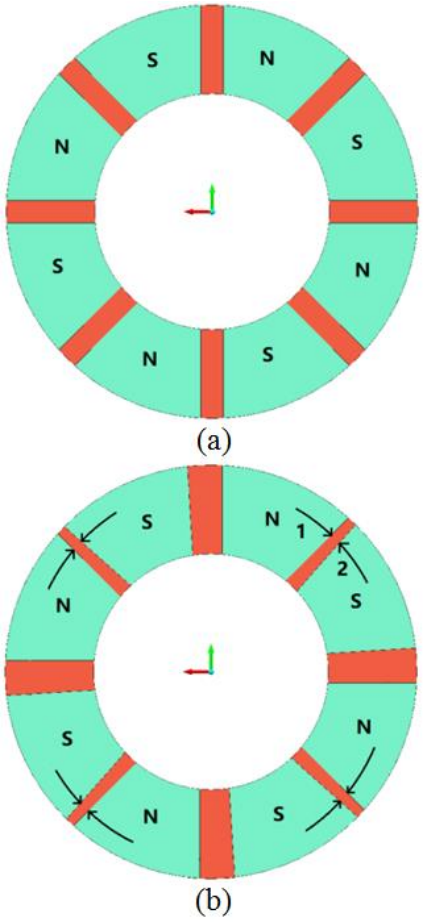

Fig 5. (a) Reference rotor design without PM shift (b) Improved rotor design with shifted PM.

Cogging torque is the sum of series of cogging torque harmonics. As a result, the cogging torque produced by a single permanent magnet can alternatively be thought of as the sum of series harmonics. Following equation represents cogging torque from each magnet.

$$T_{cogg_p} = \sum_{i=1}^{\infty} T_p N_p i \sin\left(N_p i\alpha\right) \tag{5}$$

here, T_pN_pi is per magnet coefficient. Each permanent magnet has the same relative position to respective stator slot hence considered as repeating unit and generates cogging torque that is in phase. Total cogging torque is characterized with equation 6 as under.

$$T_{cogg_p} = 2p\sum_{i=1}^{\infty} T_p N_p i \sin\left(N_p i\alpha\right) \tag{6}$$

Using neighboring k repeating units to cancel harmonics, equation 6 becomes:

$$T_{cogg_p} = \frac{1}{k}\sum_{j=0}^{k-1}\sum_{i=1}^{\infty} T_p N_p i \sin\left(N_p i\left(\alpha + j\theta\right)\right) \tag{7}$$

where, j is number of repeating units of PM, and θ is angle of magnet shifting relative to each other so as to have cancellation effect on harmonics of cogging torque given by,

$$\theta = \frac{T_n}{k} = \frac{2\pi}{N_p nk} \tag{8}$$

where, n is harmonic order of cogging torque harmonics, and T_n is the cycle time of this harmonic. With the application of right MS technique, the harmonic sum of the cogging torque of all magnets could be reduced as per equations 6 and 7. Because the magnet position is one of the key components in air-gap flux variation, it is critical to only shift magnets to obtain trapezoidal back EMF and reduced CT. Rotor magnet poles are grouped (north pole and south pole) and shifted in group in anti-clockwise and clockwise respectively as shown in the accompanyingFigure 5(b).

The reference design is shown in Figure 5(a), which does not include magnet shifting. Figure 5(b) illustrates one of the modified rotors with magnet shifted by 3.5°. It is vital to realize that just magnets are displaced while all other dimensions remain constant i.e., magnet width, rotor diameter, rotor core depth, magnet shape, magnet height, and etc.

5. RESULTS

The reference model created with the information shown in Table 1 is subjected to the Magnet Shifting approach covered in Section 4. Three dimensional (3D) FEA is used to obtain cogging torque profiles with the application of MS technique. Improved model incorporates magnets shifted by 1°, 2°, 3°, 3.5° and 4° respectively.

Compression of CT profiles of improved model with different MS values and initial motor is done to present the effectiveness of the MS technique and is displayed in Fig. 6.

It is analysed that the net CT is reduced due to shifting of rotor magnets (where north pole magnets are shifted in clockwise direction and south pole magnets are shifted in anti-clockwise direction as discussed in previous section). Table 2 indicates variation of cogging torque and average torque of AF-BLDC motor. The peak CT value of initial AF-BLDC is 5.43 N.m. while improved motor with magnet shift of 3.5° has peak CT of 3.0 N.m. This decrease in CT (peak

to peak) from 5.43 N.m. to 3.0 N.m. was achieved with just a minor compromise in average torque.

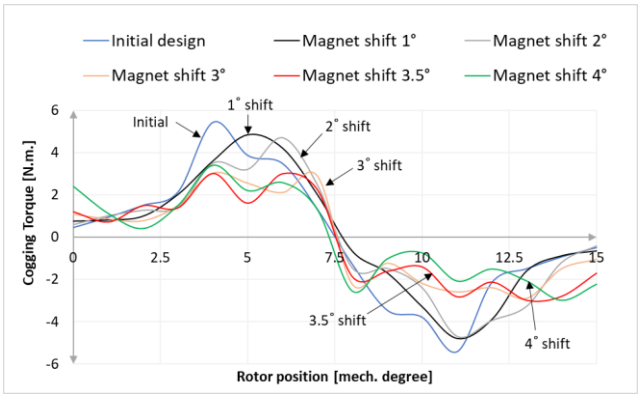

Fig. 6. CT profiles compression for different MS value (in ◦) with initial motor.

Table 2. Initial and upgraded axial flux motor design comparison

Magnet Shifting	CT		Avg. Torque		TR %
	Peak N.m.	Reduction (%)	N.m.	Reduction (%)	
0° [Initial design]	5.43	--	15.09	--	47.29
1°	4.84	10.86	14.91	1.19	40.23
2°	4.7	13.44	14.88	1.39	33.59
3°	3.05	43.83	14.82	1.78	29.0
3.5°	3.0	44.75	14.81	1.85	23.63
4°	3.41	37.20	14.85	1.59	31.64

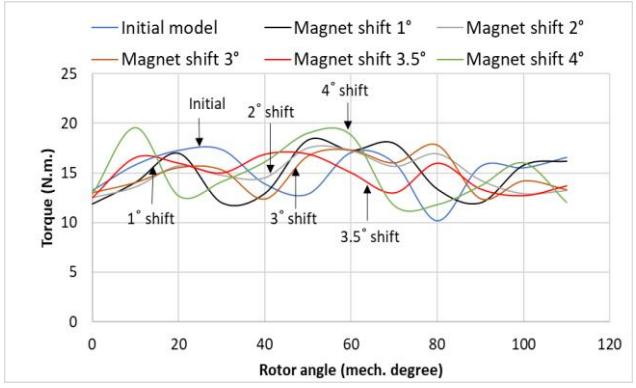

Fig. 7. Torque profiles compression for different MS value (in ◦) with initial motor.

Figure 7 depicts the torque profiles of the original motor and the improved motor with magnet shifting. The average torque of initially designed AF-BLDC is 15.09 N.m. while improved motor with magnet shift of 3.5° has average torque of 14.81 N.m. It is analyzed that reduction in cogging torque is 44.75 % with marginal reduction of 1.85 % in average torque of motor. Torque ripple (TR) is reduced from 47.29 % to 23.63 % due to design modification with magnet shifting technique. The back EMF waveforms of the initial and modified motors should be compared and analysed. As a result, fig. 8 compares the back EMF profile of the original and improved motor. It has been found that using the magnet shifting technique improves the back EMF waveform compared to using the original motor.

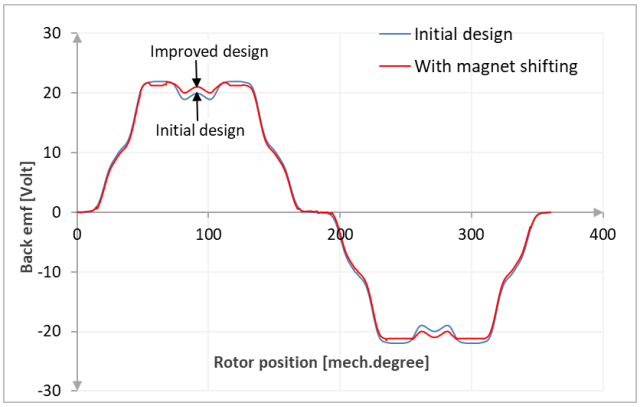

Fig. 8. Back emf waveforms of initial design and improved design.

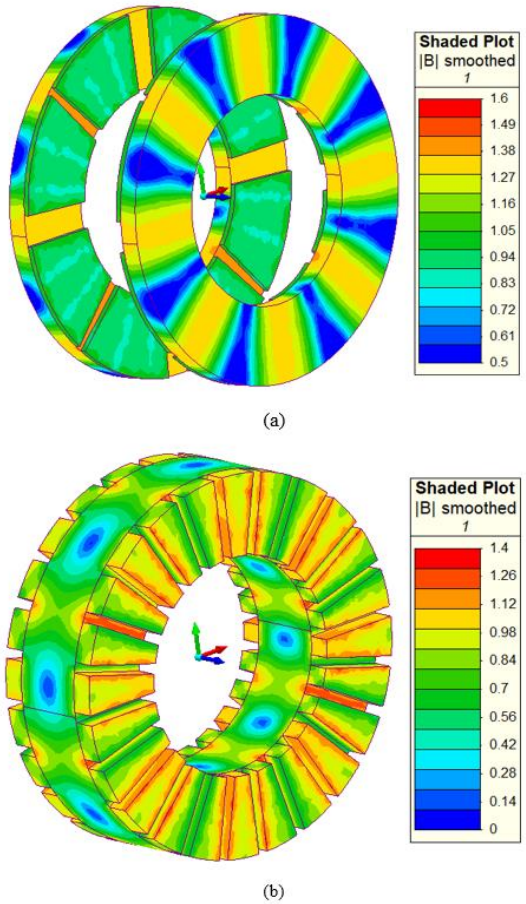

Fig. 9. Improved motor flux density profile.

It is very essential to evaluate flux density profile of reference design and improved deign. To evaluate actual flux densities in various motor parts and to validate reference & improved designs electromagnetic field analysis (EMFA) is performed. Using finite element method flux density calculation is done [26].

On the basis of anticipated performance and material characteristics, flux density is initially assumed. As flux density assumption directly affects the overall performance of motor. Improper selection can lead to saturation of material which will degrade the performance of the motor hence its evaluation is quite significant. The flux density distribution in the redesigned stator and rotor is shown in Figures 9(a) and 9(b) respectively. It has been shown that the actual flux density in various portions is very similar to the initial estimated flux densities, confirming the accuracy and efficacy of the suggested design technique.

6. CONCLUSION

Cogging torque is inherent in AF-BLDC motors and is one of the major problems for low-speed vehicular applications. Hence reduction of CT is highly desirable during design process of motor. This paper presents CT reduction of a 250 W, 150 rpm, dual rotor surface permanent magnet AF-BLDC motor. Initially reference motor was designed and EMFA is done using 3D FEA method. Magnet shifting technique is applied to the two rotors of 8 poles each to obtain the overall CT reduction. With application of proposed technique, it is analyzed that the 44.75 % reduction is achieved in peak value of CT with negligible reduction in average torque. The back EMF profile is also improved and remains symmetrical. In different motor sections, the actual flux densities closely match the corresponding predicted flux densities. Therefore, it can be said that the magnet shifting technique is a successful strategy for reduction of CT of dual rotor AF-BLDC motor and can be used for other permanent magnet motor topologies as well.

REFERENCES

[1] Yang, Y.-P.; and Chuang, D.S. 2007. Optimal design and control of a wheel motor for electric passenger cars. *IEEE Transactions on Magnetics* 43(1): 51–61.

[2] Zheng, P.; Zhao, J.; Liu, R., Tong ; and C., Wu, Q. 2010. Magnetic characteristics investigation of an axial-axial flux compound-structure pmsm used for hevs. *IEEE Transactions on Magnetics* 46(6): 2191–2194.

[3] Hung Bui Duc; Dinh Bui Minh; and Vuong Dang Quoc. 2023. Modeling of Centrifugal Stress and Deformation of Double V and Delta Layer of Interior Permanent Magnet Rotor DesignApplication to Electrical Vehicles. *GMSARN International Journal* 17:302-308.

[4] Chan, C.C. 1987. Axial-field electrical machines design and applications. *IEEE Transactions on Energy Conversion* EC-2(2): 294–300.

[5] Aydin, M., Huang, S and Lipo, T.A. 2004. Axial flux permanent magnet disc machines: A review. *Symposium on Power Electronics, Electrical Drives, Automation and Motion SPEEDAM*. Capri,Italy, 16-18 June.

[6] Cavagnino, A.; Lazzari, M.; Profumo, F.; and Tenconi, A. 2002. A comparison between the axial flux and the radial flux structures for pm synchronous motors. *IEEE Transactions on Industry Applications* 38: 1517–1524.

[7] Di Gerlando, A.; Foglia, G.; Iacchetti, M.F.; and Perini, R. 2011. Axial flux pm machines with concentrated armature windings: Design analysis and test validation of wind energy generators. *IEEE Transactions on Industrial Electronics* 58(9): 3795–3805.

[8] Hendershot, J.R.; and Miller, T.J.E. 1994. *Design of Brushless* Permanent-*magnet Motors*. Hillsboro, OH, Oxford and Magna Physics Pub. , Clarendon Press.

[9] Polat, M.; Aky¨un, Y.; and Nory, H. 2022. Minimizing the influence of cogging torque on motor performance of pm synchronous machines for elevator applications. *Arabian Journal for Science and Engineering* 47.

[10] Fei, W. and Luk, P.C.K. 2009. A new technique of cogging torque suppression in direct-drive permanent magnet brushless machines. *IEEE International Electric Machines and Drives Conference*. Miami, USA, 03-06 May.

[11] Islam, R., Husain, I.; Fardoun, A. and McLaughlin, K. 2007. Permanent magnet synchronous motor magnet designs with skewing for torque ripple and cogging torque reduction. In *IEEE Industry Applications Annual Meeting*. New Orleans, LA, USA, 23-27 September.

[12] Boukais, B.; and Zeroug, H. 2010. Magnet segmentation for commutation torque ripple reduction in a brushless dc motor drive. *IEEE Transactions on Magnetics* 46(11): 3909–3919.

[13] Liu, T.; Huang, S.; Gao, J.; and Lu, K. 2013. Cogging torque reduction by slot-opening shift for permanent magnet machines. *IEEE Transactions on Magnetics* 49(7): 4028–4031.

[14] Chabchoub, M., Ben Salah, I., Krebs, G., Neji, R. and Marchand, C. 2012. Pmsm cogging torque reduction: Comparison between different shapes of magnet. *First International Conference on Renewable Energies and Vehicular Technology*. Nabeul, Tunisia, 26-28 March.

[15] Chu, W.Q.; and Zhu, Z.Q. 2013. Investigation of torque ripples in permanent magnet synchronous machines with skewing. *IEEE Transactions on Magnetics* 49(3): 1211–1220.

[16] Zhao, W.; Lipo T.A.; and Kwon, B.-I. 2014. Material-efficient permanent-magnet shape for torque pulsation minimization in spm motors for automotive applications. *IEEE Transactions on Industrial Electronics* 61(10): 5779–5787.

[17] Zhang, B., Wang, X., Zhang, R. and Mou, X. 2008. Cogging torque reduction by combining teeth notching and rotor magnets skewing in pm bldc with concentrated windings. In *International Conference on Electrical Machines and Systems*. Wuhan, China, 17-20 October

[18] Petrov, I.; Ponomarev, P.; Alexandrova, Y.; and Pyrh¨onen, J. 2012. Unequal teeth widths for torque ripple reduction in permanent magnet synchronous machines with fractional-slot non-overlapping windings. *IEEE Transactions on Magnetics* 51(2): 1–9.

[19] Dosiek, L.; and Pillay, P. 2007. Cogging torque reduction in permanent magnet machines. *IEEE Transactions on Industry Applications* 43(6): 1565–1571.

[20] Upadhayay, P. and Rajagopal, K.R. 2013. Torque ripple reduction using magnet pole shaping in a surface mounted permanent magnet bldc motor. 2*013 International Conference on Renewable Energy* Research *and pplications (ICRERA)*. Madrid, Spain, 20-23 October.

[21] Aydin, M.; and Gulec, M. 2014. Reduction of cogging torque in double-rotor axial-flux permanent-magnet disk motors: A review of cost-effective magnet-skewing techniques with experimental verification. *IEEE Transactions on Industrial Electronics* 61(9): 5025–5034.

[22] Jahns, T.M.; and Soong, W.L. 1996. Pulsating torque minimization techniques for permanent magnet ac motor drives - A review. *IEEE Transactions on Industrial Electronics* 43(2): 321–330.

[23] Park, G.-J.; Kim, Y.-J.; and Jung, S.-Y. 2016. Design of ipmsm applying v-shape skew considering axial force distribution and performance characteristics according to the rotating direction. *IEEE Transactions on Applied Superconductivity* 26(4): 1–5.

[24] Kumar, P. and Srivastava, R.K. 2018. Cost-effective stator modification techniques for cogging torque reduction in axial flux permanent magnet machines. *IEEE Transportation Electrification Conference and Expo, Asia-Pacific (ITEC Asia-Pacific).* Bangkok, Thailand, 06-09 June.

[25] Huang, S.; Luo, J.; Leonardi, F.; and Lipo, T.A. 1998. A general approach to sizing and power density equations for comparison of electrical machines. *IEEE Transactions on Industry*
Applications 34(1): 92–97.

[26] Raja Ram Kumar; Chandan Chetri; Priyanka Devi; and R.K. Saket. 2021. Design and Analysis of Novel Dual Stator Hybrid Operational Six-Phase Permanent Magnet Synchronous Machine for Wind Power Application. *GMSARN International Journal* 15: 211 – 216.